JOURNAL OF MATERIALS SCIENCE 28 (1993) 2353–2360

Sol–gel processing of titanium-containing thin coatings

Part I *Preparation and structure*

B. SAMUNEVA, V. KOZHUKHAROV, Ch. TRAPALIS
Sofia University of Technology, Sofia - 1756, Bulgaria

R. KRANOLD
Wilhelm-Pieck Universität - Rostock, Rostock, Germany

Using tetrabutylorthotitanate as a precursor, titanate coatings with and without modifiers such as SnO_2 and Fe_2O_3 have been successfully obtained. The hydrolysis and polycondensation mechanism is discussed in relation to the sol–gel transition. The gel-formation region was obtained as well as stable-layer formation and phase-separation regions in the $Ti(OBu^n)_4$–C_2H_5OH–H_2O system. Coatings deposited on glass substrates exhibited a strong tendency to aggregate and with increasing temperature to crystallize in anatase or rutile phases (500 and 1000 °C, respectively). Structural characteristics of the gel products were investigated by SEM, X-ray and electron diffraction measurements, as well as by small-angle X-ray scattering. It was established that after thermal treatment at 500 °C for 10 min, spherical aggregates were formed in the coatings, having an average radius of approximately 5.1 nm.

1. Introduction

After the pioneering work of Dislich [1], synthesis of glassy materials by the sol–gel technology has proved to be an interesting and quickly developing scientific field [2]. It has been shown that through this technology glasses may be synthesized with compositions hitherto thought impossible to achieve through standard methods of melting. Thin vitreous or polycrystalline layers are also new products obtained through the sol–gel method. By varying the content of TiO_2, for example, coatings of high refractive index in combination with other applicable properties may be deposited [3]. Introducing modifiers is frequently used to increase chemical resistance [4, 5] to achieve additional colouring effect [6, 7] or to obtain a definite transmittance and reflection [8] of the layers. Mono-TiO_2 coatings have been investigated in detail by Nogami and Moria [9] to establish their infrared transmittance. Yamamoto *et al.* [10] investigated thin-film preparation with compositions from the binary SiO_2–TiO_2 system drawn from alkoxide solutions. Strawbridge and James [11] investigated in detail the dipping process in sol solutions of $Ti(OEt)_4$ and C_2H_5OH. The basic characteristics of the process are described in Dislich's publications [12–14].

It is known that the sol–gel process is a suitable technology to prepare vitreous products of high homogeneity and purity. This is achieved by mixing the starting components at the molecular level in the sol solution. High homogeneity and the lack of impurities allow excellent physical and chemical parameters of the coatings to be achieved. Coating properties are strongly influenced by the conditions of sol preparations, by the rate of the hydrolysis and polycondensation processes, by the modifiers, viscosity, pH and H_2O/C_2H_5OH ratio, etc.

Titanium oxides prove to be of the greatest practical value compared to other oxides applied in sol–gel technology. This is mostly due to their high refractive index, good chemical stability, high electrical resistance, interesting catalytic and other properties [15–18].

The present paper presents results of investigations on processing and structural characteristics of titanate thin coatings deposited on glass substrates through the sol–gel technology. Bearing in mind the detailed experimental data on titanate layers, the facts have been presented in three separate papers, this being more appropriate and rational. This approach provides the opportunity to present results in a better way (Part II, XPS-study, and Part III Properties [19,20]) which enables the reader selectively to chose knowledge according to his personal interests. The object of the investigation is common to all three parts, so they interrelate to give a full description of the synthesis, structural characteristics, chemical analysis and properties of the titanate coatings.

2. Experimental procedure

2.1. Sol solution preparation

The process includes dissolution of titanium alkoxide as $C_{16}H_{36}O_4Ti$ and the respective salts in a chosen solvent, followed by hydrolytic polycondensation

0022–2461

TABLE I Compositions of titanium-containing sol solutions

Composition	$Ti(OBu^n)_4$ (mol %)	C_2H_5OH (mol %)	H_2O (mol %)	Second component (mol %)	Composition of oxide in coatings (wt %)	
001	3.0	97.0	–	–	100	TiO_2
002	3.0	85.0	12.0	–	100	TiO_2
004	4.5	95.0	–	0.5	82.54	TiO_2
				($SnCl_4$)	14.96	SnO_2
005	15.0	75.0	5.0	5.0	61.40	TiO_2
				($SnCl_4$)	38.60	SnO_2
007	15.0	75.0	5.0	5.0	60.0	TiO_2
				($Fe(NO_3)_3 \cdot 9H_2O$)	40.0	Fe_2O_3
009	10.0	82.0	3.0	5.0	66.7	TiO_2
				($Fe(NO_3)_3 \cdot 9H_2O$)	33.3	Fe_2O_3

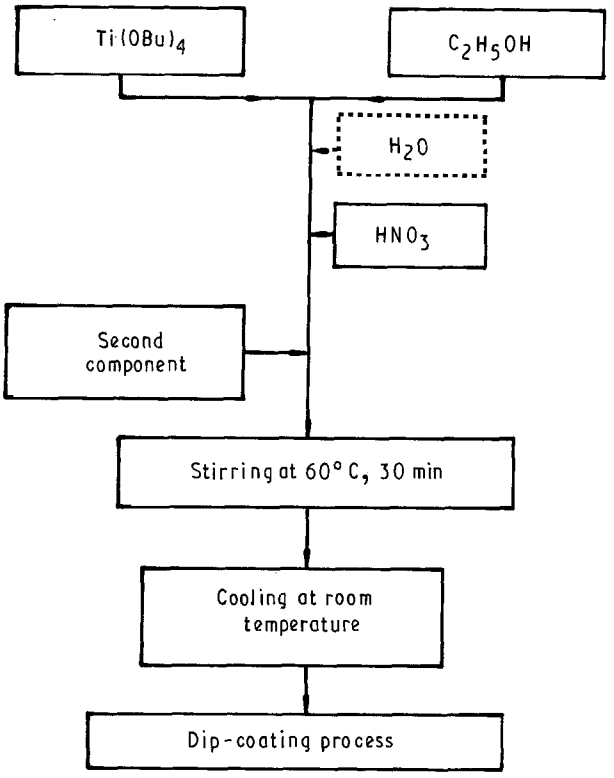

Figure 1 Sol–gel processing of TiO_2-containing thin films from $Ti(OBu^n)_4$ used as the precursor.

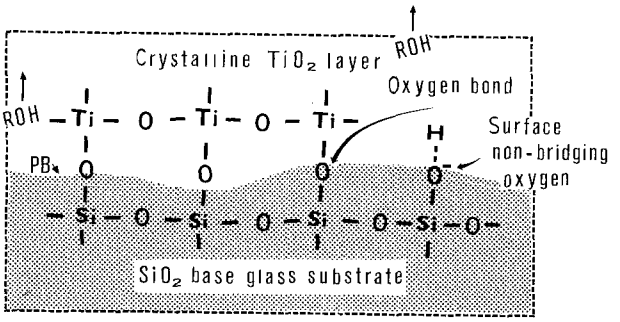

Figure 2 Adhesion of the metal oxide (TiO_2) film to the glass surface. PB, phase boundary

leading to the preparation of a multicomponent and transparent solution which polymerizes in the course of time. All compositions investigated are listed in Table I. They are calculated with the respective mole(weight) per cents of the initial constituents and of the related final oxide products with the help of the BATHR computer program [21].

The starting substance was tetrabutylorthotitanate (TBTi or $Ti(OBu)_4$) from Merk. Modifiers were introduced in alcoholic solutions of nitrates or chlorides of the respective metals of high purity (p.a.).

Fig. 1 shows a block diagram of the preparation of thin layers used in our study. The sol and the respective gel products were prepared as follows: the calculated quantity of ethyl alcohol was dropped through a pipette into a vessel suitable for the purpose, and then $Ti(OBu^n)_4$ was added. During moderate mixing by a magnetic stirrer, water was added drop by drop according to the calculations, so that the hydrolysis process takes place. At the end of the process the system was a monophase and transparent solution. Some drops of concentrated nitric acid were added in the ratio $HNO_3/TBTi = 0.01$, as catalyst of hydrolysis. At a moderate stirring rate the system was heated to 60 °C for 30–60 min. In that time the second component (acid, nitrate, chloride) was added in the respective quantities. Polymerization occurred during the course of which the final titanate-containing transparent solution was obtained. After a short ageing, depending on the conditions, the system was transformed into a transparent gel product. Gel-formation is not a desirable process in thin-layer processing, so various steps were undertaken to stabilize the sol solution, for example, addition of stabilizers and organic additives or maintaining low concentrations of the initial constituents. Low concentrations of the film-forming components in the sol solution may be guaranteed by using compositions rich in ethyl alcohol and lacking in water, which enables a suitable viscosity of the solution (below 10 cP) to be maintained. It was established that solutions with a viscosity over 10 cP produce microcracks in the coatings during thermal treatment. A high stability of the sol solutions with time is achieved at a pH value between 1 and 4.

2.2. Deposition of layers

Thin layers of chosen composition (see Table I) characterize high stability of the titanium-containing sol solutions which were of interest because of their physical and chemical properties, were deposited on flat

glass-type Flasch Glas A.G. The glass substrates had excellent parallelity and flatness. They were cleaned using the technology of the Central Laboratory of Photoprocesses at BAS, which included the following steps: ultrasonic water treatment, deionized water treatment, surface active substances solution treatment, alcohol treatment and drying in a dry nitrogen flow. Dipping was done following the method described in detail by Dislich [12].

2.3. Methods

SEM investigations were carried out in a Jeol JSM-T200 using secondary electrons (SEI regime) and back-scattered electron images in compositional contrast (COMPO regime). To improve the surface conductivity of layers a standard vacuum evaporation procedure with gold was applied.

Phase identification of the thin layers was made using an X-ray diffractometer, type TUR M62, Germany. The X-ray source was CuK_α radiation of $\lambda = 0.154\,20$ nm. Calculation and comparison of the X-ray diffraction values was made with the help of personal computer, Pravetz-16 and VAX-770 with JCPDS data base [22].

Some of the samples deposited on polymer plastic folio placed on the substrate, were tested after thermal treatment, using the Debye-Scherer method with CuK_α radiation. The photometering of Debyegrams was performed with a photometer type TENNO, Trento, Italy. Another group of samples was investigated using a Rigaku-Denki X-ray diffractometer, Japan, using small-angle X-ray scattering (SAXS) at MoK_α radiation of $\lambda = 0.07107$ nm and scattering angle, θ, corresponding to $0.3\ nm^{-1} \leqslant s \leqslant 31\ nm^{-1}$, where s may be expressed by [23].

$$s = \frac{4\pi}{\lambda}\sin\left[\frac{\theta}{2}\right] \tag{1}$$

3. Chemistry of the process

The main chemical reactions taking place are as follows

$$Ti(OR)_4 + 4H_2O \longrightarrow Ti(OH)_4 + 4ROH\uparrow \tag{2a}$$

$$Ti(OH)_4 \xrightarrow{t} TiO_2 + 2H_2O\uparrow \tag{2b}$$

As hydrolysis proceeds polycondensation of the hydrolysis products takes place according to the reactions

$$xTi(OR)_2(OH)_2 \longrightarrow$$

$$\begin{array}{l} -Ti(OR)_2-O-Ti(OR)_2-Ti(OR)_2-O- \xrightarrow[-ROH]{+H_2O} \\ \quad\ | \qquad\qquad\qquad\quad | \\ -Ti(RO)-O-Ti(OR)-O-Ti(OR)-O- \xrightarrow[-H_2O]{+\Delta T} \\ \qquad\qquad\qquad\qquad | \\ \qquad\qquad\qquad\quad OH \end{array}$$

$$\begin{array}{c} OR \\ | \\ -Ti(RO)_2-OTi-O-Ti(RO)_2-O- \\ | \\ HO-Ti-O-Ti(RO)_2- \\ | \\ OR \end{array} \tag{3}$$

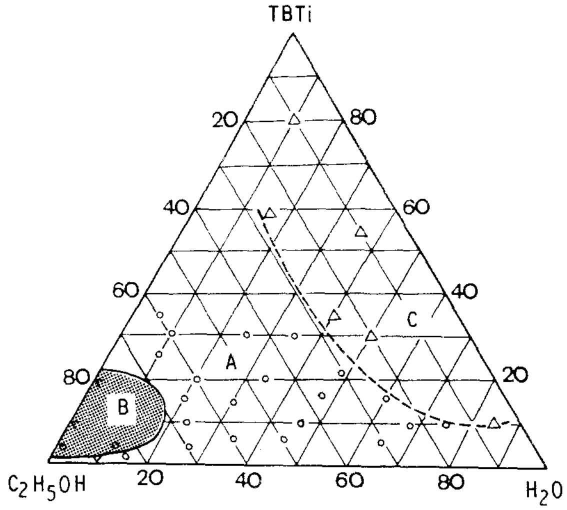

Figure 3 Regions in the $Ti(C_4H_9O)_4$–C_2H_5OH–H_2O system; region A is the gel-forming region; region B (shaded area) is the dip-coating region; region C is the immiscible region

To obtain oxide layers of good optical and mechanical properties, hydrolysis and polycondensation must proceed slowly and simultaneously. In time, the hydrolysis is suppressed, while the polycondensation becomes stronger, being stimulated by the next thermal treatment. Good adhesion of the layer to the glass substrate results from the surface reaction of some building groups with the glass surface. The glass SiO_2-base network also penetrates the layer in this way. A simple schematic diagram of this process is presented in Fig. 2.

4. Results and discussion

4.1. Gel-formation region determination

Sakka *et al.* [24–26] followed the acidic catalysed hydrolytic polycondensation of tetraethylorthosilicate and proved that the low water concentration caused spiral bonding of polymeric chains in the sol, thus forming a solution, ready for the drawing of fibres. The same authors [27] studied gel formation of siloxanes with different functional groups and defined the regions of gel-formation, phase separation and non-gelling homogeneous solution. Duran *et al.* [6] investigated the properties of glassy layers in the SiO_2–M_xO_y system, where M is iron, cobalt, iron + cobalt, and outlined the area of compositions appropriate for qualified drawing of thin layers in the TEOS–EtOH–H_2O system.

No data have been found in the literature referring to gel-formation region determination in the $Ti(OBu^n)_4$–EtOH–H_2O system. The present work aimed to define the gel-formation region in this system. Fig. 3 shows a summary of the experimental results obtained for 30 ml solutions, for the respective geometrical points after the treatment described above. Region C was characterized by a liquid separation and precipitation took place at a very high speed. Here hydrolysis products (titanate hydroxides) rapidly spoil the homogeneity, transparency and stability of the solution, thus resulting in crystalline-phase formation.

To keep the titanate sol solutions stable for a long period of time and ready to be drawn in thin layers, it is recommended that researchers work with compositions in region B, even without water. Hydrolysis, necessary for the gel-film formation, is accomplished under the influence of atmospheric moisture, sometimes over 80%, due to the high hydrosorption ability of the titanium butoxide and its respective sol solutions.

4.2. SEM investigations

From the experimental data for stable gel-formation regions and the drawing of layers (see Fig. 3, regions A and B, respectively) the compositions in Table I for the coatings obtained, were characterized by SEM.

Fig. 4a shows a scanning electron micrograph of a gel titanate coating of composition 001 (surface regions with microdefects were specially selected, because the layers obtained were very smooth). The same coating but at a different angle of observation, is shown in Fig. 4b. A nonuniform band, typical of the coating after thermal treatment, is clearly seen.

4.3. X-ray and electron diffraction study

Fig. 5 shows X-ray diffraction patterns of a titanate gel product. It is seen that for the layer deposited and dried at 120 °C for 10 min, no crystalline phase exists, while at higher temperatures a crystalline phase is seen. At much higher temperatures, a phase transition of anatase (500 °C) to rutile and brookite phase (1000 °C) is dominant.

A similar picture is typical for samples of code 005 and 007 whose diffractograms are presented on Figs. 6 and 7, respectively. With increasing temperature, a co-crystallization of titanium oxide and the oxide-modifier SnO_2 takes place (see Fig. 6). The crystallization process is less obvious for the sample treated at 500 °C, but is very evident for the sample treated at 1000 °C. On increasing the temperature of samples to 500 °C in the system TiO_2–Fe_2O_3, two co-existing crystalline phases TiO_2 and $TiO_2 \cdot Fe_2O_3$ are found. After a thermal treatment at 1000 °C for 1 h, intensive crystallization takes place. Data are available concerning the presence of the compound $TiFe_2O_5$ coexisting with the high-temperature TiO_2 modification [22].

The initial X-ray diffraction investigations of thin coatings on glass substrates did not, in fact, indicate the presence of a crystalline phase, perhaps because of lack of mass, therefore it was necessary to use the Debye–Scherer method. Data from electron diffraction investigations show the presence of kind of short-range order in coatings containing TiO_2 and TiO_2 plus SnO_2 (Figs 8 and 9). Coatings treated by the Debye–Scherer method were separated from the polymer substrate before thermal treatment (separation of the coating from the glass substrate was impossible because of its strong adhesion). The Debyegrams and the photometric spectra are presented on Figs 8, 9 and 10 marked as D.

Fig. 8 shows data from the phase characterization of the crystal coating of mono-TiO_2 (code 001). It is seen

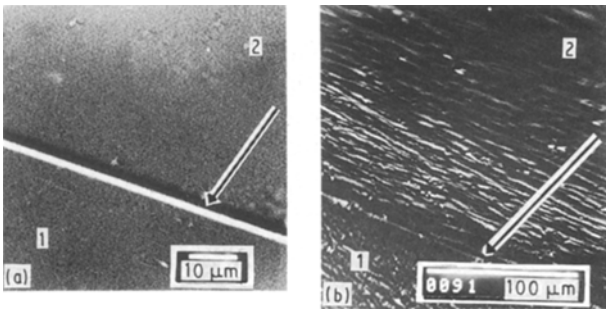

Figure 4 Cross-sectional view scanning electron micrographs of a coating of composition 001, (a) before thermal treatment, where (1) is the glass substrate and (2) is the coating (regime COMPO), and (b) after thermal treatment at 500° C, 10 min, where (1) is the glass substrate and (2) is the TiO_2 coating microview under an angle of observation of 40° (regime SEI). Phase-boundary substrate/coating is arrowed.

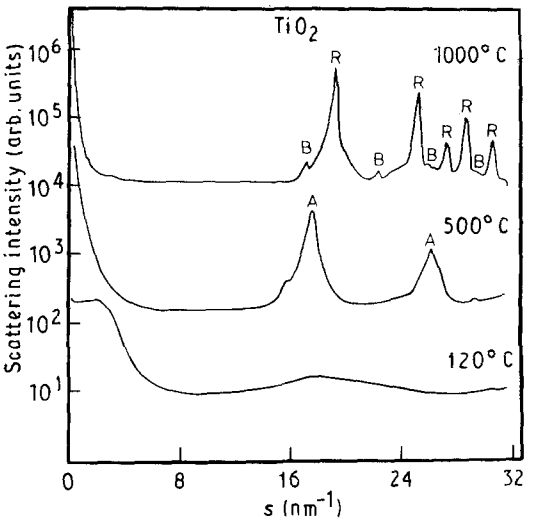

Figure 5 X-ray diffraction curves of the gel product with code 002 after thermal treatment for 1 h. A, Anatase; B, brookite; R, rutile.

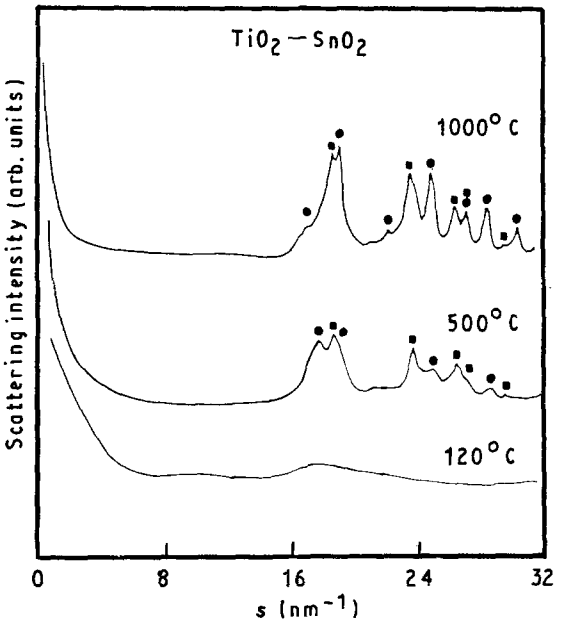

Figure 6 X-ray diffraction curves of the gel product with code 005 after thermal treatment at 120, 500 and 1000° C for 1 h. (●) TiO_2, (■) SnO_2.

that the coatings have an even surface. The X-ray picture of the coating deposited on the glass-substrate (curve R) shows X-ray vitreous phase. After the electron diffraction study it was established that the coating was polycrystalline (Fig. 8E). The presence of crystalline TiO_2 as anatase phase, was checked in the layer separated from the polymer substrate (see Fig. 8, curve D) heated at 500 °C for 10 min.

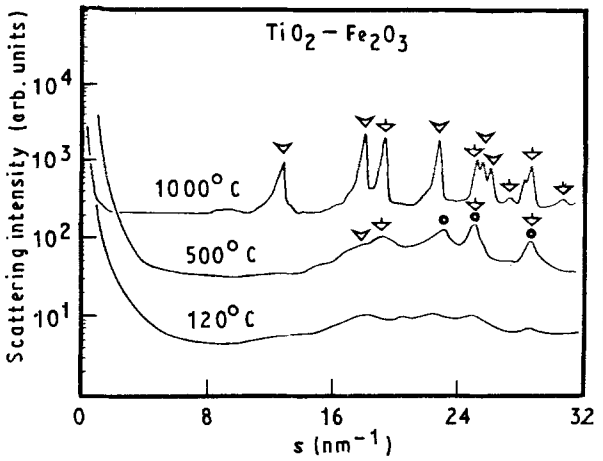

Figure 7 X-ray diffraction curves of the gel product with composition 007 containing Fe_2O_3 after thermal treatment for 1 h. (▽) TiO_2, (▽) $TiO_2 \cdot Fe_2O_3$, (○) α-Fe_2O_3.

Results from the investigation of a coating of composition 004 are presented in Fig. 9. It is noticed that the thin film separated from the polymer substrate has a crystalline anatase phase. However, using X-ray phase analysis, no crystalline phase was detected (Fig. 9, curve R) which may be due to the negligible mass of the coating and its very small thickness. The micrograph shows the presence of microcracks in the layer, possibly caused by the initiation of internal tension during thermal treatment.

Fig. 10 shows the results after characterization of the coating with composition 007. On separation from the polymer substrate, the coating crystallizes in the anatase phase and α-Fe_2O_3 after thermal treatment at 500 °C for 10 min.

4.4. SAXS studies

To clarify the microaggregate process in the coatings, the layers were obtained investigated using small-angle X-ray scattering. From the experimental SAXS curves through the least square method, the radii of the microaggregates present in the volume was estimated without any collimation correction. The data

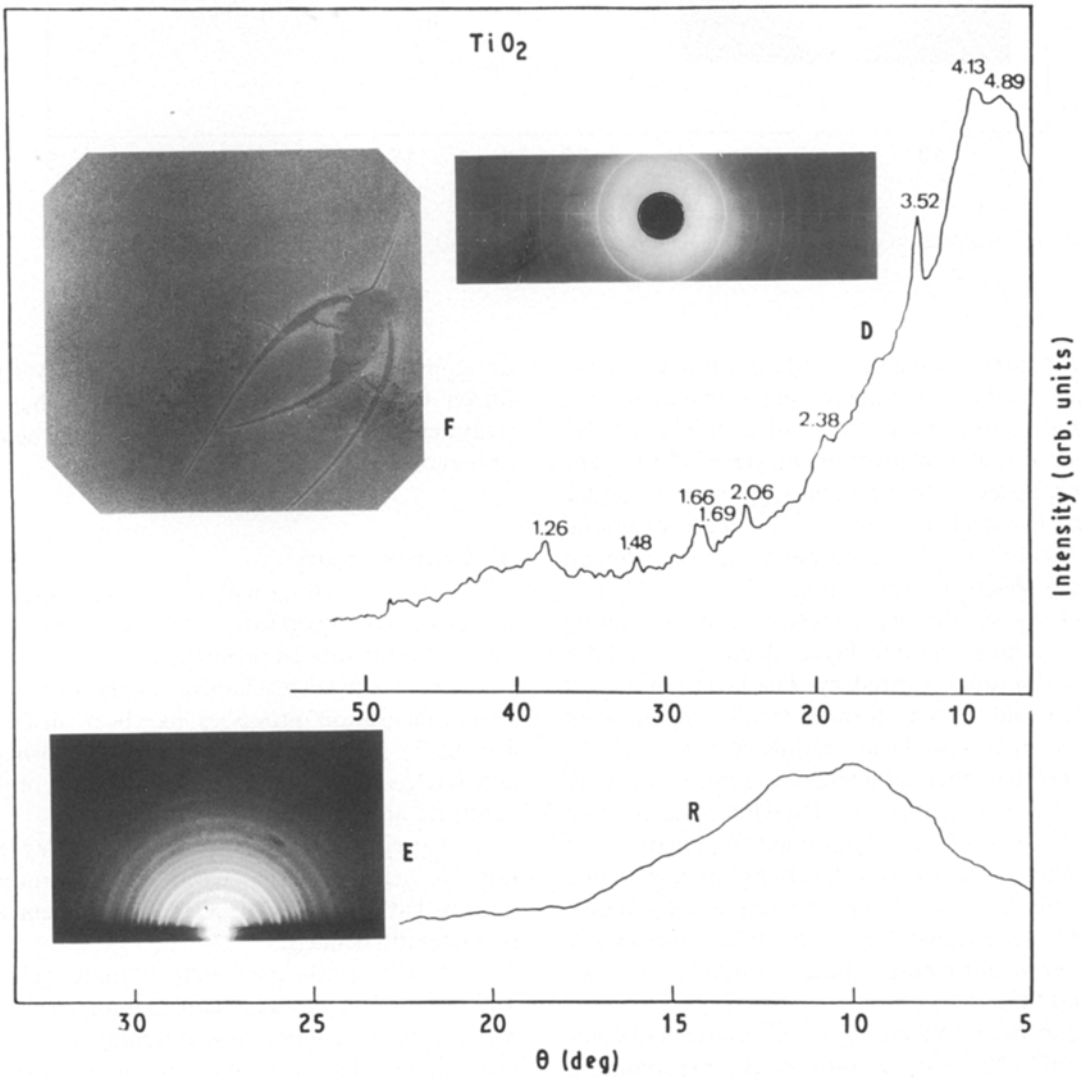

Figure 8 Phase characteristics of the TiO_2 thin film, code 001, after thermal treatment at 500 °C, 10 min. (R) X-ray diffraction patterns, (D) Debyegram, (E) electron diffraction surface micrograph, and (F) planar view of the film surface.

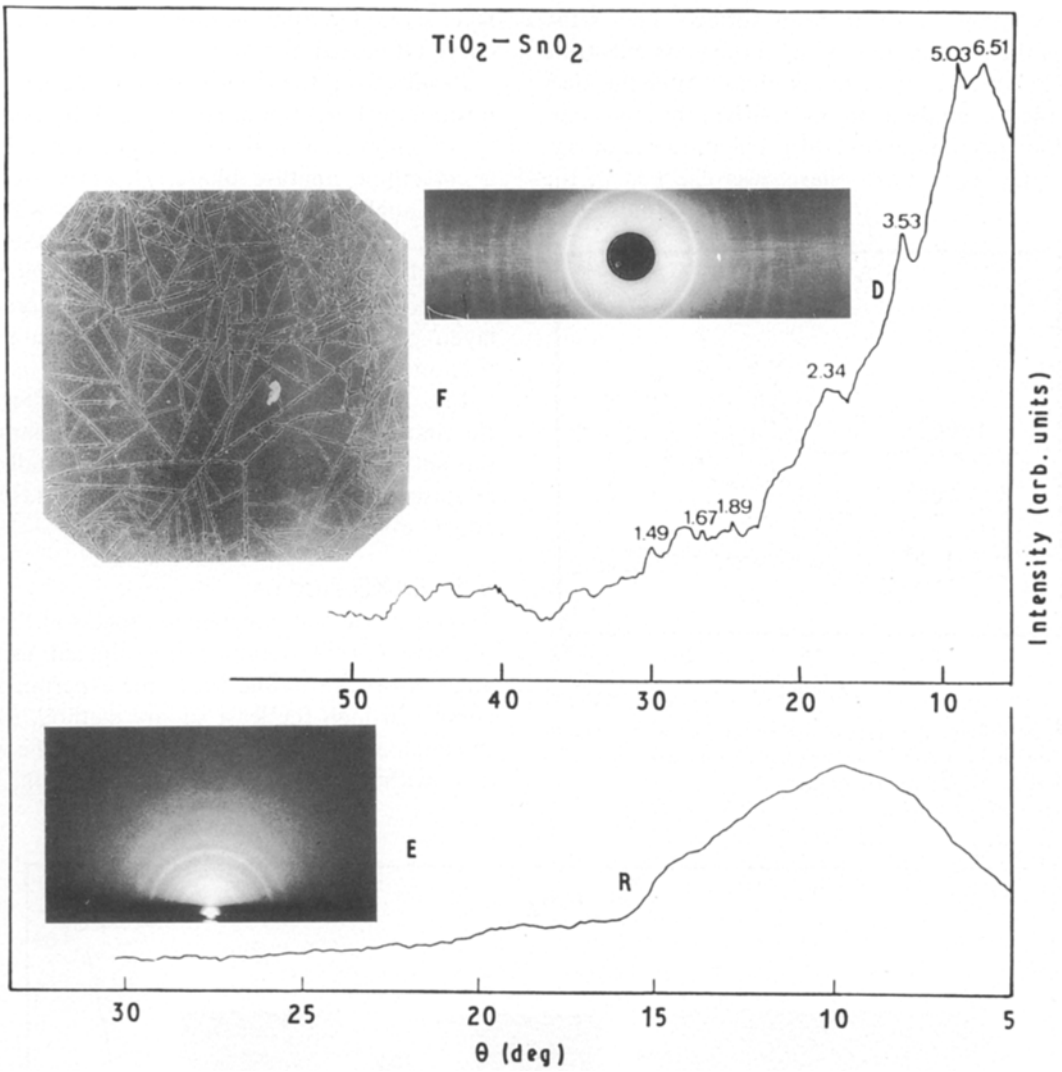

Figure 9 Phase characteristics of the titanium-containing coating with code 004; R, D, E and F, see in Fig. 8.

show that samples had a fine crystalline fracture structure, which tend to agglomerate on thermal treatment. (Of interest to us are the studies of Zarzycki [28–31] on the structural investigation of gel products. The author proposes a simple fracto-aggregation model, according to which the clusters and microstructural formations are formed continuously, starting from an elementary spherical aggregation radius [29, 30].)

Fig. 11 shows the experimental X-ray scattering curve for a monotitanate layer, deposited on both sides of a thin quartz capillary. The layer consists of aggregated and already formed small crystallites of TiO_2 of average correlation radius $\bar{R}_g \simeq 4.3$ nm. ($\bar{R}_g$ depends on the spherical aggregation radius through the formula $R = (5/3\bar{R}_g)^{1/2}$.) Therefore, the titanate coating consists of already formed aggregations of TiO_2, of almost spherical clusters of radius $R \approx 5.1$ nm. These fracto-aggregates could be accepted as microcrystalline formations of TiO_2 from the X-ray and electron diffraction phase analysis data (see Figs 8 and 9).

Fig. 12 shows SAXS curves of gel products of composition 002. The average radii of the predominant clusters in the gels treated at 120 and 500 °C, respectively, are approximately 0.96 and 5.5 nm. This shows development of gel aggregation, in the layer with the higher temperature. It was established that thermal treatment densifies the coating structure which is built of bigger aggregations.

5. Conclusions

1. Titanate coatings with or without modifiers were successfully obtained from alcoholic solutions of tetrabutylorthotitanate as precursor.

2. The chemical mechanism of the hydrolysis and polycondensation processes has been discussed for $Ti(OBu^n)_4$, as well as the manner of formation of adhesive oxide bonds between the surface of the glass substrate and the sol → gel → oxide layer.

3. The regions of gel formation, stable layer formation, as well as phase separation of solution in the ternary $Ti(OC_4H_9)_4$–C_2H_5OH–H_2O system were experimentally defined.

4. It was established that titanate gels exhibit a strong tendency to aggregate and for crystal growth with increasing temperature of treatment. The crystalline phase identified after thermal treatment at 500 °C is anatase, while at 1000 °C it is mainly rutile phase.

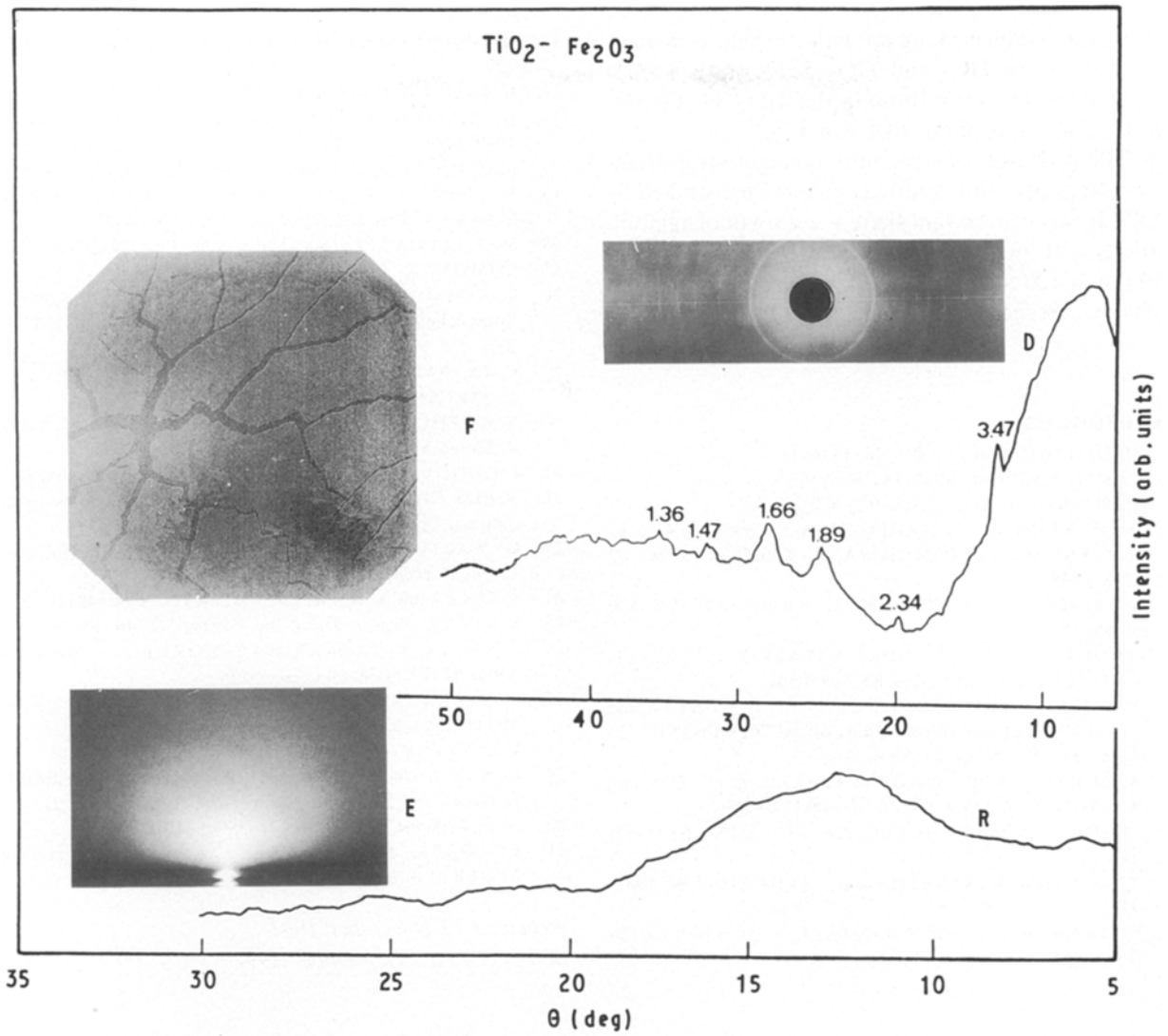

Figure 10 Phase characteristics of TiO_2–Fe_2O_3 thin film with code 007; R, D, E and F, see in Fig. 8.

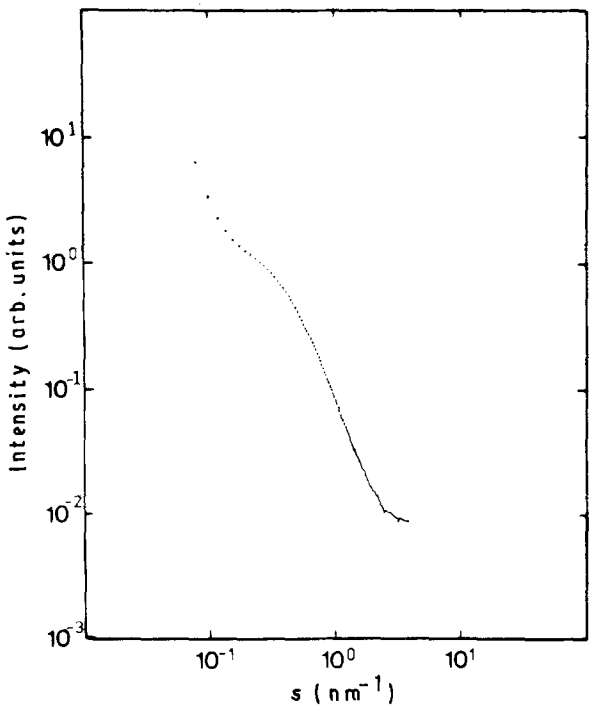

Figure 11 SAXS curve for TiO_2 coating on a quartz glass substrate after treatment at 500° C; composition 001.

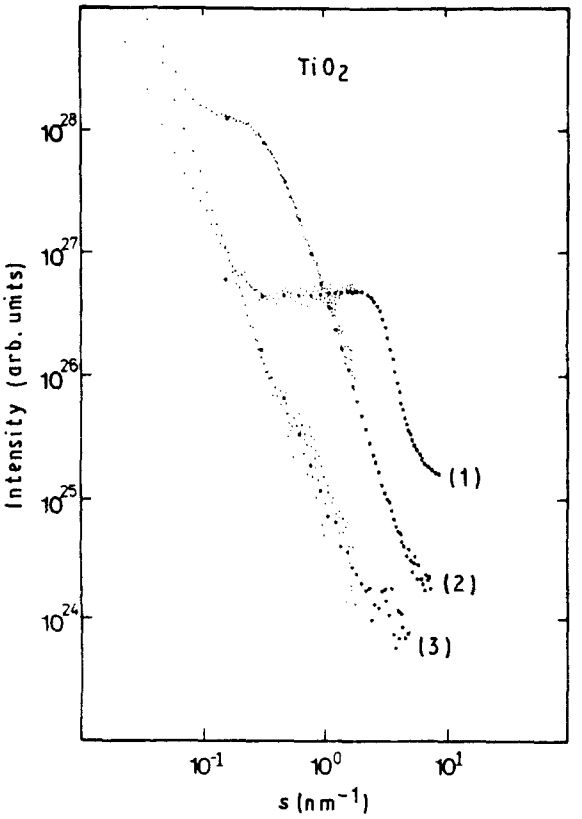

Figure 12 SAXS curve for gel products with composition 002 after thermal treatment at (1) 120° C, (2) 500° C and (3) 1000° C for 1 h.

5. It was established, again with the help of X-rays, that coatings on TiO_2 and TiO_2–SnO_2 show a tendency to devitrify, while those in the TiO_2–Fe_2O_3 system have an amorphous-like structure.

6. The processes of structural aggregation in titanate coatings over thin quartz capillary were studied by SAXS. It was proved that there is a growth of agglomerations with increasing treatment temperature from 0.96 nm at 120 °C up to approximately 5.1 ± 0.5 nm at 500 °C, respectively.

References

1. H. DISLICH, *Glastech. Ber.* **44** (1971) 1.
2. *Idem, J. Non-Cryst. Solids* **73** (1985) 599.
3. H. SCHROEDER, *Opt. Acta* **9** (1962) 249.
4. A. MAKISHIMA, H. OOHASHI, M. WAKAKUWA, K. KOTANI and T. SHIMOHIRA, *J. Non-Cryst. Solids* **42** (1980) 549.
5. W. BEIER, A. GOEKTAS and G. FRISCHAT, *ibid.* **100** (1988) 531.
6. A. DURAN, J. FERNANDEZ-NAVARRO, P. CASARIEGO and A. JOGLAN, *ibid.* **82** (1986) 301.
7. V. KOZHUKHAROV, S. NIKOLOV, B. SAMUNEVA and CH. TRAPALIS, in "Proceedings of the 7th CIMTEC", 24 June 1991, Vol. 67 (Satel. Simp. Al.).
8. A. DURAN, J. FERNANDEZ-NAVARRO, P. MAZON and A. JOGLAR, *J. Non-Cryst. Solids* **100** (1988) 494.
9. M. NOGAMI and Y. MORIA, *Yogyo-Kyokai Shi* **85** (1977) 448.
10. Y. YAMAMOTO, K. KAMIA and S. SAKKA, *ibid.* **90** (1982) 328.
11. I. STRAWBRIDGE and P. JAMES, *J. Non-Cryst. Solids* **86** (1986) 381.
12. H. DISLICH and E. HUSSMAN, *Thin Solid Films* **77** (1981) 129.
13. H. DISLICH, *Glastech. Ber.* **57** (1984) 229.
14. H. DISLICH, P. HINZ and N. ARFFSTEN, "Sol–Gel 1969–1989", in XV International Congress on Glass, Leningrad, Vol. 2a Ed. O. Hazurim (Nauka, Leningrad, 1989) p. 52.
15. T. YOKO, K. KAMIYA, A. YUASA, K. TANAKA and S. SAKKA, *J. Non-Cryst. Solids* **100** (1986) 483.
16. M. VILLEGAS, *Bol. Soc. Esp. Cerám. Vidr.* **29** (1990) 315.
17. I. THOMAS, *Appl. Opt.* **26** (1987) 4688.
18. G. SAMSONAV (ed.) "Fiziko-khimicheskie svoistva okislov, Spravochnik", (Metallurgia, Moscow, 1978) pp. 124, 204, 214, 235.
19. C. TRAPALIS, V. KOZHUKHAROV, B. SAMUNEVA and P. STEFANOV, *J. Mater. Sci.*, **28** (1993) 1276.
20. V. KOZHUKHAROV, C. TRAPALIS and B. SAMUNEVA, *J. Mater. Sci.*, **28** (1993) 1283.
21. I. GUGOV, BATHR program, unpublished results (1988).
22. JCPDS X-ray Powder data base, Inorganic Phases (International Center for Diffraction Data, PA, 1981).
23. G. WALTER, R. KRANOLD and U. LIMKE, *Macromol. Chem. Macromol. Symp.* **15** (1988) 361.
24. S. SAKKA and K. KAMIYA, *J. Non-Cryst. solids* **48** (1982) 31.
25. S. SAKKA, *Reprint Trans. Ind. Ceram. Soc.* **46** (1987) 1.
26. S. SAKKA, Y. TANAKA and T. KOKUBO, *J. Non-Cryst. Solids* **82** (1986) 24.
27. S. SAKKA, K. KAMIYA, K. MAKITA and Y. YAMAMOTO, *ibid.* **63** (1984) 223.
28. J. ZARZYCKI, *ibid.* **93** (1987) 173.
29. *Idem*, in "Science of Ceramic Chemical Processing", edited by L. Hench and D. Ulrich (Wiley, New York, 1986) p. 21.
30. *Idem, J. Non-Cryst. Solids* **121** (1990) 110.
31. T. LOARS, J. ZARZYCKI, A. CRAIERICH and M. AEGERTER, *ibid.* **121** (1990) 216.

Received 12 December 1991
and accepted 2 September 1992